

# A microfluidic impedance biosensor based on immunomagnetic separation and urease catalysis for continuous-flow detection of *E. coli* O157:H7

Lan Yao<sup>a</sup>, Lei Wang<sup>b</sup>, Fengchun Huang<sup>b</sup>, Gaozhe Cai<sup>b</sup>, Xinge Xi<sup>c</sup>, Jianhan Lin<sup>a,b,\*</sup>

<sup>a</sup> Key Laboratory of Agricultural Information Acquisition Technology, Ministry of Agriculture, China Agricultural University, Beijing 100083 China

<sup>b</sup> Key Laboratory on Modern Precision Agriculture System Integration Research, Ministry of Education, China Agricultural University, Beijing 100083, China

<sup>c</sup> Department of Biological and Agricultural Engineering, University of Arkansas, Fayetteville, AR 72701, USA



## ARTICLE INFO

### Article history:

Received 16 October 2017

Received in revised form

11 December 2017

Accepted 18 December 2017

Available online 19 December 2017

### Keywords:

Impedance biosensor

Impedance normalization

Continuous-flow detection

Immunomagnetic separation

Urease catalysis

## ABSTRACT

Early screening of foodborne pathogens is a key to control the outbreaks of foodborne illnesses. In this study, a microfluidic impedance biosensor combined with the immune magnetic nanoparticles (MNPs) for bacteria separation, the urease for biological signal amplification and the microfluidic chip for impedance measurement was developed for rapid, sensitive and continuous-flow detection of *E. coli* O157:H7. After the streptavidin modified MNPs were conjugated with the biotinylated polyclonal antibodies (PAb) to form the immune MNPs, the target bacteria was first separated by the MNPs from the background to form the MNP-bacteria complexes. Then, the gold nanoparticles (GNPs) modified with the urease and the aptamers against *E. coli* O157:H7 were conjugated with the MNP-bacteria to form the MNP-bacteria-GNP-urease complexes. Finally, the complexes were used to catalyze the hydrolysis of urea into ammonium carbonate, leading to the decrease in the impedance. The impedance was online measured by this proposed biosensor and analyzed using the impedance normalization to determine the concentration of *E. coli* O157:H7. A good linear relationship between the impedance relative change rate of the catalysts and the concentration of the bacteria was obtained with low detection limit of 12 CFU/mL.

© 2017 Elsevier B.V. All rights reserved.

## 1. Introduction

Foodborne pathogens have drawn great public attention worldwide, since they could lead to serious healthy issues and significant economic losses. It was estimated by World Health Organization (WHO) that 600 million people (almost 1 in 10) in the world fell ill after eating contaminated foods and 42 million died every year, resulting in the loss of 33 million healthy life years [1]. The U.S. Department of Agriculture (USDA) estimated that foodborne illnesses cost \$15.6 billion in the U.S. every year [2]. In China, it was reported by National Healthy and Family Planning Commission (NHFPC) that 5926 people suffered from food poisoning in 2015

and the major cause of food poisoning was foodborne pathogens, including *Salmonella*, *Vibrio parahaemolyticus*, *Bacillus cereus*, *Staphylococcus aureus* and *Escherichia coli*, etc. [3]. Rapid screening of foodborne pathogens in foods has become one of the major challenges in preventing the outbreaks of foodborne illnesses. Thus, rapid, sensitive and online detection methods for screening the contaminated foods in their supply chains are urgently needed to ensure food safety.

Currently available methods for bacteria detection mainly include culture plating (Culture), polymerase chain reaction (PCR), and enzyme-linked immune-sorbent assay (ELISA), etc. Culture is the gold standard method with high reliability and sensitivity, however it is very time-consuming. PCR is a rapid, sensitive and high throughput method [4,5], however it has high requirements on nucleic acid extraction and well-trained technician. ELISA is also a rapid and high throughput method [6,7], however it often lacks sufficient sensitivity and has false positives. As alternative, various types of biosensors, such as optical [8–10], electrochemical [11,12],

\* Corresponding author at: Key Laboratory of Agricultural Information Acquisition Technology, Ministry of Agriculture, China Agricultural University, Beijing 100083 China.

E-mail address: [jianhan@cau.edu.cn](mailto:jianhan@cau.edu.cn) (J. Lin).

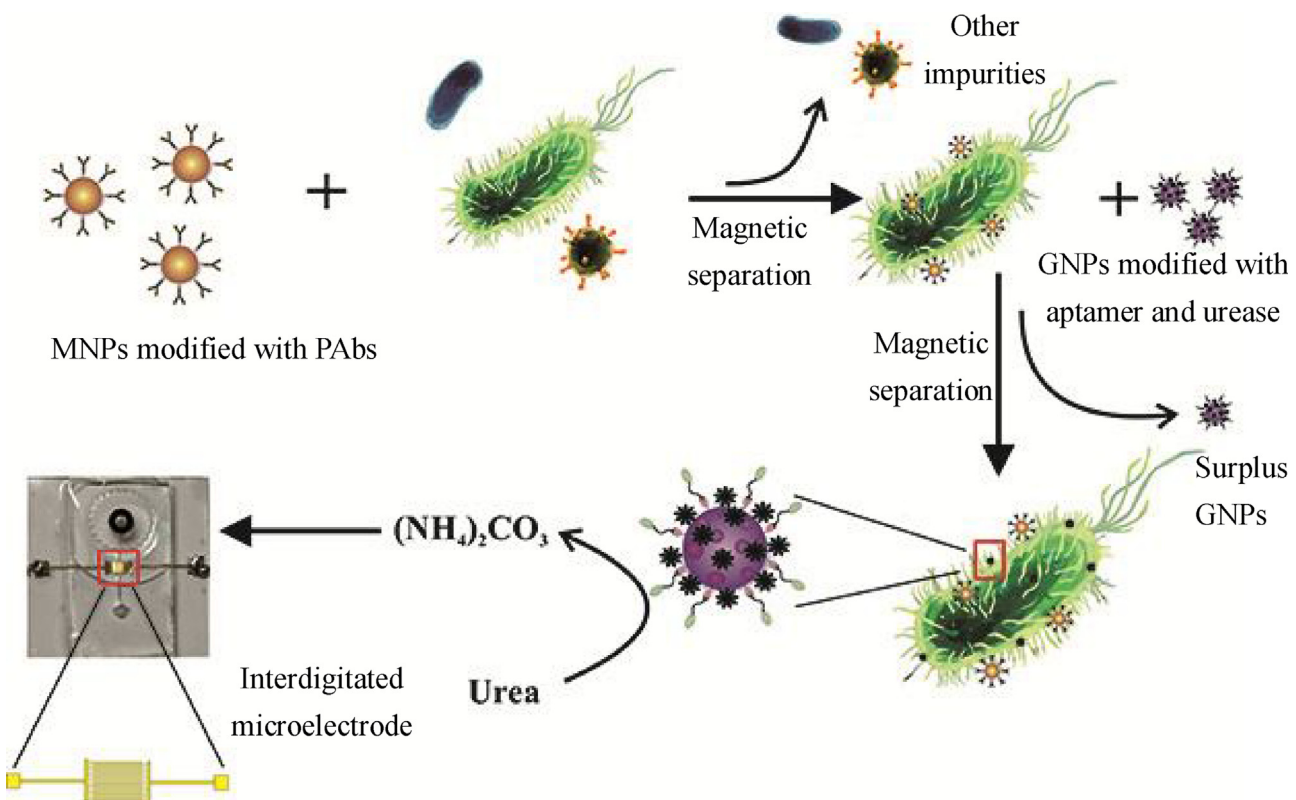


**Fig. 1.** The principle of the microfluidic impedance biosensor based on immunomagnetic separation and urease catalysis for continuous-flow detection of *E. coli* O157:H7.

magnetic [13,14], quartz crystal microbalance [15,16] and surface plasmon resonance [17,18], etc., have been reported for rapid and sensitive detection of foodborne pathogens. Impedance biosensor is one type of electrochemical biosensors and relies on the electrochemical impedance change on the interface of the electrode under an alternating perturbation with a direct-current bias. It is often featured with compact design, easy integration, rapid response and low cost, and interdigitated array microelectrodes with low ohmic drop, high signal-to-noise ratio and miniature size are often used as transducer. Besides, impedance biosensor is often combined with immune magnetic separation for specific isolation and efficient concentration of biological targets from complex sample background. Magnetic nanoparticles (MNPs) own high surface-to-volume ratio, less steric hindrance and uniform distribution, and are often modified with the antibodies against the target for reacting with the targets, followed by applying an external magnetic field to capture the MNP-target complexes and remove the sample background. To the best of our knowledge, there is few study reporting online detection of foodborne pathogens, however it is needed in some links in the food supply chains, such as milk and poultry processing, etc.

In our previous study [19], we have successfully developed a fluidic separation chip with active magnetic mixing for online isolation and concentration of *Listeria monocytogenes* with the separation efficiency of ~90% in 30 min. Besides, we also have developed a microfluidic detection chip with interdigitated array microelectrode for quantitative measurement of impedance change with the linear detection range of the catalysate (ammonium carbonate) from 1 μM to 100 μM. However, the impedance was measured in the static condition, i.e., the catalysate was measured ~10 min after it was injected into the detection chip, resulting in longer detection time, worse background noise control and lower sensitivity. Besides, the microelectrodes fabricated even in the same batch often had an unsatisfied uniformity in the

impedance measurement of the catalysate at the same concentrations. In this study, we intended to develop a microfluidic impedance biosensor for continuous-flow detection of foodborne pathogenic bacteria using immunomagnetic separation for isolating and concentrating the target bacteria from the sample background, urease catalysis for amplifying the biological signals, and continuous-flow impedance measurement for determining the concentration of the bacteria. Besides, we used *E. coli* O157:H7 as research model to verify and evaluate this proposed biosensor. As shown in Fig. 1, after the streptavidin modified MNPs were conjugated with the biotinylated polyclonal antibodies (PAb) against *E. coli* O157:H7 through streptavidin-biotin binding to form the immune MNPs, they were used for magnetic separation of the target *E. coli* O157:H7 cells in the sample to form the MNP-PAb-bacteria complexes (magnetic bacteria). Then, the gold nanoparticles (GNPs), modified by the aptamers against *E. coli* O157:H7 and the urease, were incubated with the magnetic bacteria to form the MNP-PAb-bacteria-aptamer-GNP-urease complexes (enzymatic bacteria). The urea was catalyzed by the urease on the enzymatic bacteria and hydrolyzed into the catalysate (ammonium carbonate), resulting in an increase in the ion strength and thus a decrease in the impedance. The impedance of the catalysate was measured at the continuous-flow condition using the improved microfluidic detection chip with the gold interdigitated array microelectrode and analyzed using the impedance normalization method to determine the concentration of the bacteria in the sample.

## 2. Materials and methods

### 2.1. Materials and reagents

Streptavidin, biotin, urea ( $\text{NH}_2\text{CONH}_2$ ), ammonium carbonate ( $(\text{NH}_4)_2\text{CO}_3$ ), urease (E.C.3.5.1.5, Type III, 15,000–50,000

units/g solid), and 2-(N-morpholino) ethanesulfonic acid (MES) were purchased from Sigma Aldrich (St. Louis, MO, USA). The biotinylated polyclonal antibodies against *E. coli* O157:H7 were purchased from Thermo Scientific (Waltham, MA, USA) for specifically reacting with the *E. coli* O157:H7 cells. The aptamers against *E. coli* O157:H7 were synthesized by Sangon Biotech (Shanghai, China) with the sequence of 5'-biotin-CCGGACGCCATTGCCTGCCATCTACAGAGCAGGTGTGACGG-3'.

The streptavidin conjugated magnetic nanoparticles with the diameter of 150 nm from Ocean Optics (MHS-150-10, Dunedin, FL, USA) were used for immunomagnetic separation of the target bacteria. Gold chloride tri-hydrate (HAuCl<sub>4</sub>·3H<sub>2</sub>O) from Sigma Aldrich (St. Louis, MO, USA) was used to synthesize the gold nanoparticles with the diameter of ~20 nm. Phosphate buffer saline (PBS, P5493, diluted 10 times by deionized water to 10 mM, pH 7.4) was also purchased from Sigma Aldrich. Bovine serum albumin (BSA) from Sigma Aldrich and polyethylene glycol (PEG) 20,000 from Merck (Darmstadt, Germany) were prepared in PBS for blocking. Tween-20 was obtained from Amresco (Solon, OH, USA) for washing the non-specific binding impurities. The deionized water produced by Millipore Advantage 10 (18.2 MΩ·cm, Billerica, MA, USA) was used to prepare all the solutions.

## 2.2. Fabrication of the microfluidic detection chip

The microfluidic detection chip was fabricated by bonding the redesigned glass-substrate interdigitated array gold microelectrode and the microfluidic channel. The gold microelectrode included 25 pairs of digit fingers with 15 μm digit width, 15 μm inter-digit spacing, 3 mm digit length and 100 nm thickness. Chromium with the thickness of 10 nm was used as the connecting layer. The microfluidic channel with 100 μm height, 1 mm width and 3 mm length was fabricated based on 3D printing and PDMS casting. The 3D drawing in.stl format was designed using Solid-works software and the mold was printed by the 3D printer (Vero Whiteplus RGD835, Stratasys, Eden Prairie, MN, USA). The PDMS prepolymer and curing agent were mixed at the ratio of 10:1 for 5 min and degassed for 20 min in vacuum. Then, the mixture was poured into the mold and placed at 60 °C overnight. After the PDMS channel and the glass-substrate microelectrode were treated by surface plasma (Harrick Plasma, Ithaca, NY, USA), they were bonded to form the microfluidic chip. Besides, the microfluidic channel was intercrossed vertically with the digit fingers of the microelectrode instead of being parallel with the fingers in our previous design. Compared to the previous detection chip, the improved chip required less catalysate for impedance measurement due to 3 times smaller channel size, and could be fabricated more easily due to much lower requirement on the alignment of the PDMS channel and the microelectrode.

## 2.3. Culture and enumeration of the bacteria

*Escherichia coli* O157:H7 (ATCC43888, used as target bacteria), *Salmonella typhimurium* (ATCC14028, used as non-target bacteria) and *Listeria monocytogenes* (ATCC13932, used as non-target bacteria) were stored at -20 °C with glycerol and revived by streaking on Luria-Bertani (LB) agar plates. First, they were cultured in the LB medium (Aoboxing Biotech, Beijing, China) at 37 °C for 12–16 h with shaking at 180 rpm, respectively. Then, the cultures were serially 10-fold diluted by PBS to obtain the bacteria at the concentrations from 10<sup>1</sup> to 10<sup>5</sup> CFU/mL, respectively.

For bacterial enumeration, the bacterial samples were serially diluted with the sterile PBS, and 100 μL of the diluents were surface plated on the LB agar plates. After incubation at 37 °C for 22–24 h, the colonies were counted to calculate the concentration of the bacteria.

## 2.4. Surface modification of the GNPs

The synthesis of the GNPs with the size of ~20 nm had been reported in our previous paper with slight adjustment [20]. The aptamers against *E. coli* O157:H7 and the urease were modified onto the GNPs to form the aptamer and urease modified GNPs (apta-urease GNPs). Briefly, the pH of the GNPs was first adjusted to 7.0 with 0.2 M K<sub>2</sub>CO<sub>3</sub>. Then, streptavidin (1 mg/mL) was added drop-by-drop into the GNPs and incubated for 1 h. After the biotinylated aptamers (10 μM) and the urease (10 mg/mL, in 5 mM MES, prepared by the deionized water) were added drop-by-drop and incubated for 5 min and 1 h, respectively, the GNPs were successively blocked by 1% (w/v) PEG for 30 min and 10% (w/v) BSA for 30 min. When streptavidin, aptamers, urease, PEG and BSA were added into the GNPs and incubated respectively, they were gently blended using magnetic stirring to achieve better reaction. Finally, the GNPs were centrifuged at 10,000 rpm for 15 min to remove the excessive aptamers and urease, and the apta-urease GNPs were dissolved in the deionized water and stored at 4 °C for further use.

## 2.5. Separation and detection of the target bacteria

The separation and concentration of the target *E. coli* O157:H7 cells from the sample (either the pure culture or the spiked milk) were based on our previously reported immunomagnetic separation method [21]. Prior to test, the immune MNPs (1 mg/mL) were prepared by mixing the streptavidin conjugated MNPs with the biotinylated PAbs (0.4–0.5 mg/mL) at 15 rpm for 45 min and magnetically separating the immune MNPs using a magnetic separator (MS0406, Abit Biotech, Jiangyin, China) for 2 min to remove the excessive PAbs. 20 μg of the immune MNPs were first incubated with 500 μL of the sample containing different concentrations (10<sup>1</sup>–10<sup>5</sup> CFU/mL) of *E. coli* O157:H7 at 15 rpm for 45 min to form the MNP-PAb-bacteria complexes (magnetic bacteria). After magnetic separation to remove the sample background, the magnetic bacteria were resuspended in 100 μL of PBST (PBS with 0.05% Tween-20) and the purified and 5 times concentrated bacteria were obtained.

The detection of the target *E. coli* O157:H7 cells is based on urease catalysis and continuous-flow impedance measurement. The separated and concentrated magnetic bacteria were incubated with 5 μL of the apta-urease GNPs at 15 rpm for 45 min to form the MNP-PAb-bacteria-aptamer-GNP-urease complexes (enzymatic bacteria). Then, the enzymatic bacteria were magnetically separated to remove the excessive apta-urease GNPs and washed with the deionized water containing 0.05% Tween-20 twice and the deionized water twice, respectively, to further remove the residual conductive ions. Finally, the enzymatic bacteria were resuspended and incubated in 100 μL of the urea with the concentration of 100 μM at 15 rpm, followed by magnetic separation for 2 min, and the supernatant including the catalysate (ammonium carbonate) and the surplus substrate (urea) was collected for impedance measurement.

## 2.6. Continuous-flow impedance measurement of the catalysate

The supernatant was continuously injected into the microfluidic impedance detection chip using the precise syringe pump (Type: T60-S2&WX10-14-A, flow rate: 0–24 mL/min, Longer Pump, Baoding, Hebei, China) at the flowrate of 1 mL/h. The impedance of the catalysate was measured every 2 s using the IM6 electrochemical workstation (ZAHNER, Kronach, Bavaria, Germany) with the Thales analysis software by applying a sinusoidal alternating potential with the amplitude of 5 mV, the direct-current bias of 0 V and the frequency range of 1 Hz–5 MHz on the microelectrode in the detection chip.

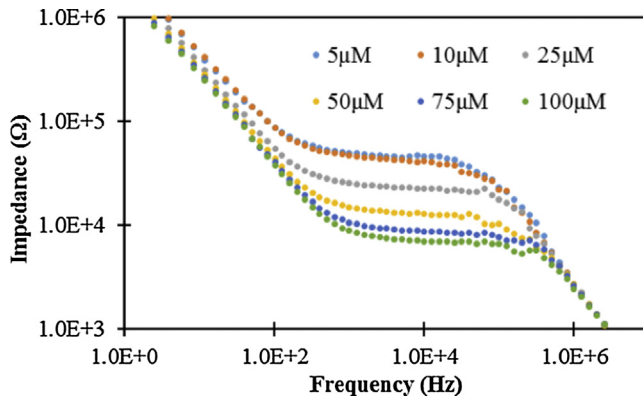


**Fig. 2.** The electrochemical impedance spectra of ammonium carbonate at different concentrations ranging from 5  $\mu\text{M}$  to 100  $\mu\text{M}$ .

Since the variation of different microelectrodes has great impact on the impedance measurement, the impedance normalization, i.e. the relative change rate of impedance (RZ) at the characteristic frequency, was used to analyze the impedance data, which was calculated by

$$\text{RZ} = (\text{Z}_u - \text{Z}_s)/\text{Z}_u \times 100\% \quad (1)$$

where,  $\text{Z}_s$  and  $\text{Z}_u$  are the impedance of the sample and the urea at the characteristic frequency, respectively.

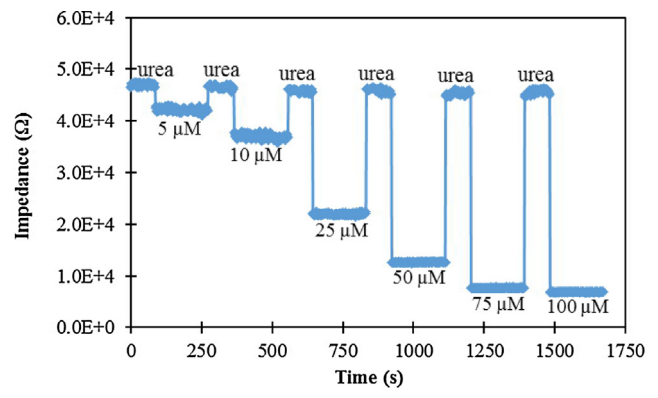
### 3. Results and discussions

#### 3.1. Analysis of the electrochemical impedance spectra

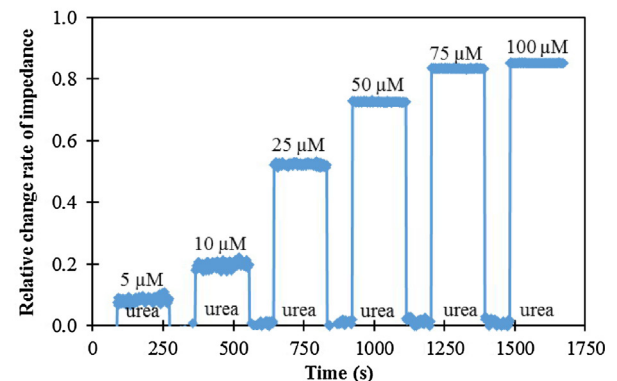
This proposed impedance biosensor was based on the continuous-flow measurement of the impedance of the catalysate (ammonium carbonate) at the presence of the urea, resulting from the hydrolysis of the urea by the urease on the enzymatic bacteria. To obtain the characteristic frequency for the continuous-flow impedance measurement, the electrochemical impedance spectra (EIS) of different concentrations (5–100  $\mu\text{M}$ ) of ammonium carbonate were measured using the IM6 electrochemical station for the proof of the concept. Fig. 2 shows the EIS for different concentrations of ammonium carbonate at the concentrations ranging from 5  $\mu\text{M}$  to 100  $\mu\text{M}$ , which were measured when they were continuously flowing through the detection chip at the flow rate of 1 mL/h. It could be seen that the impedance of ammonium carbonate increased when the concentration of ammonium carbonate decreased from 100  $\mu\text{M}$  to 5  $\mu\text{M}$ . Besides, the maximum impedance change in the EIS appeared at the frequency range from 1 kHz to 30 kHz. Therefore, the characteristic frequency was selected as 15 kHz in this study.

#### 3.2. Continuous-flow measurement of the catalysate

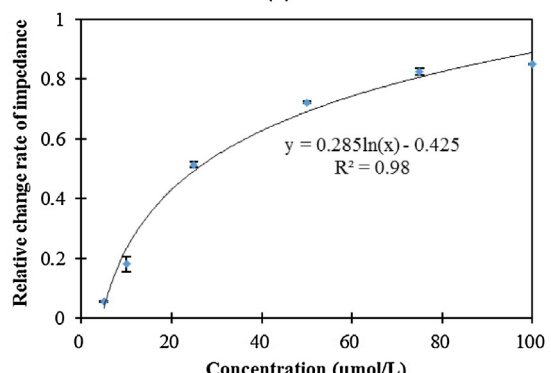
The purpose of this study was to verify the feasibility of this proposed biosensor for continuous-flow detection of the target bacteria. The continuous-flow measurement of the catalysate is the pre-condition. Thus, different concentrations (5–100  $\mu\text{M}$ ) of ammonium carbonate were used to simulate the catalysate and successively injected into the detection chip from low concentration to high concentration, and the impedance at the characteristic frequency of 15 kHz was collected every 2 s. Prior to the tests on ammonium carbonate, the urea at the concentration of 100  $\mu\text{M}$  was injected into the detection chip for washing and used as control. After each concentration of ammonium carbonate was measured, the chip was thoroughly washed with the urea till the impedance



(a)



(b)



(c)

**Fig. 3.** (a) The impedance measured at the characteristic frequency of 15 kHz in the continuous-flow condition for ammonium carbonate with the concentrations ranging from 5  $\mu\text{M}$  to 100  $\mu\text{M}$  and the urea with the concentration of 100  $\mu\text{M}$ ; (b) The relative change rate of impedance for ammonium carbonate with the concentrations ranging from 5  $\mu\text{M}$  to 100  $\mu\text{M}$  and the urea with the concentration of 100  $\mu\text{M}$ ; (c) The linear relationship between the relative change rate of impedance and the concentration of ammonium carbonate ( $N=3$ ).

returned to the original level (the first measurement of the urea). As shown in Fig. 3(a), the impedance of each concentration almost remained the same level and decreased from 42.2 k $\Omega$  to 6.9 k $\Omega$  when the concentration of ammonium carbonate increased from 5  $\mu\text{M}$  to 100  $\mu\text{M}$ , indicating that more conductive ions (ammonium ions and carbonate ions) resulted in higher conductivity and thus smaller impedance in the continuous-flow condition. Besides, the relative change rate of impedance was also calculated and shown in Fig. 3(b) and (c), RZ increased from 0.09 to 0.85 when the concentration of ammonium carbonate changed from 5  $\mu\text{M}$  to 100  $\mu\text{M}$ , and a good linear relationship between the relative change rate of

impedance (RZ) and the concentration (C) was found and could be expressed as

$$RZ = 0.285\ln(C) + 0.425 (R^2 = 0.98) \quad (2)$$

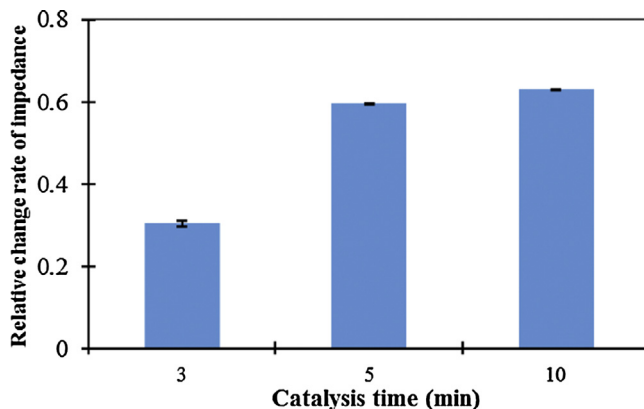


**Fig. 4.** The relative change rate of impedance measured at the characteristic frequency of 15 kHz for different enzymatic catalysis times in the detection of *E. coli* O157:H7 with the concentration of  $10^2$  CFU/mL ( $N=3$ ).

### 3.3. Optimization of the enzymatic catalysis time

The enzymatic catalysis time has a great impact on the sensitivity of this proposed biosensor. Thus, the enzymatic bacteria at the concentration of  $10^2$  CFU/mL were incubated in the urea at the fixed concentration of  $100 \mu\text{M}$  for different enzymatic catalysis times (3 min, 5 min and 10 min). The EIS of their catalysate was measured using the detection chip, and their relative change rates of impedance at the characteristic frequency of 15 kHz were calculated for comparison. As shown in Fig. 4, RZ increased from 0.30 to 0.60 while the enzymatic catalysis time changed from 3 min to 5 min. This was mainly because more ammonium carbonate was produced in the supernatant with more catalysis time for the same amount of the enzymatic bacteria to catalyze the hydrolysis of the non-conductive urea. Besides, when the catalysis time increased to 10 min, RZ only had slight increase (0.62). Therefore, the enzymatic catalysis time was optimized to be 5 min in this study.

### 3.4. Calibration curve of this biosensor for target bacteria detection

The calibration curve of this proposed impedance biosensor is the basis for quantitative determination of unknown concentration of target bacteria. Thus, different concentrations of the pure *E. coli* O157:H7 cells ranging from  $1.2 \times 10^1$  CFU/mL to  $1.2 \times 10^5$

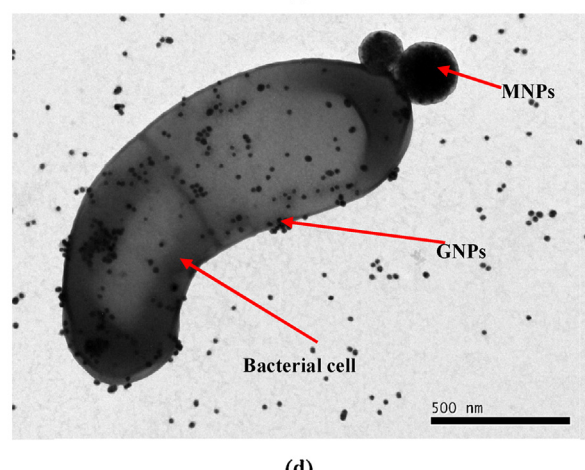
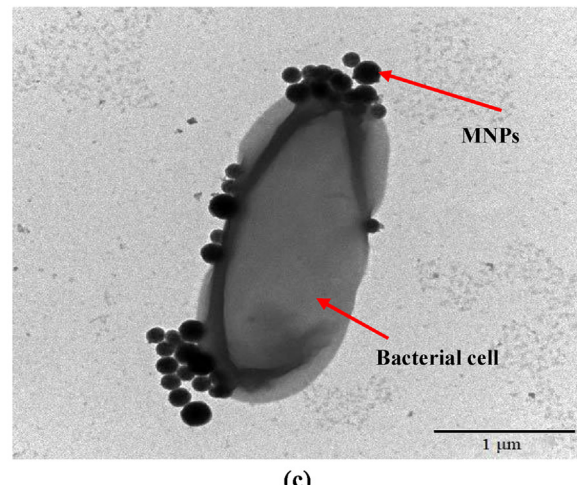
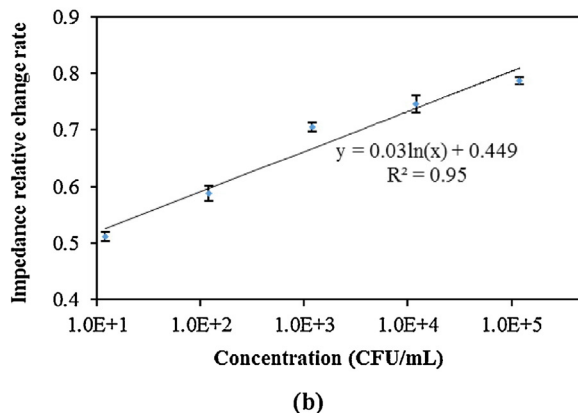
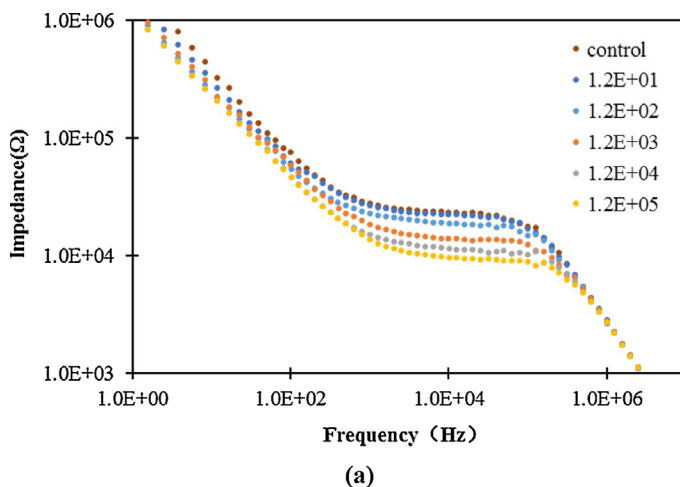


**Fig. 5.** (a) The electrochemical impedance spectra of *E. coli* O157:H7 with different concentrations ranging from  $1.2 \times 10^1$  CFU/mL to  $1.2 \times 10^5$  CFU/mL and negative control (PBS); (b) The linear relationship between the relative change rate of impedance and the concentration of *E. coli* O157:H7 ( $N=3$ ); (c) The forming of the MNP-bacteria complex; (d) The forming of the MNP-bacteria-GNP complex.

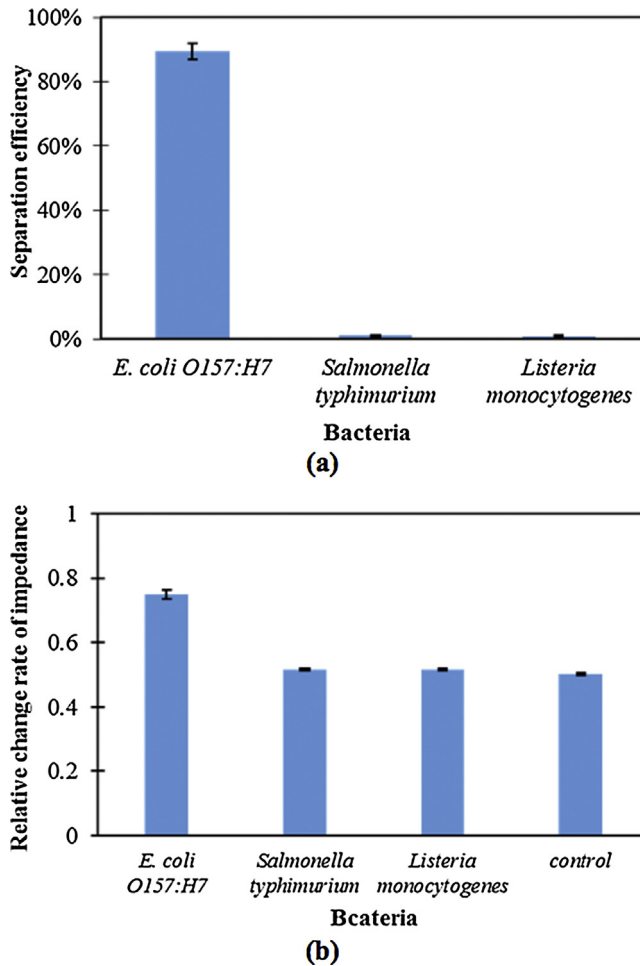


**Fig. 6.** (a) The separation efficiency of the target bacteria, *E. coli* O157:H7, and the non-target bacteria, *Salmonella* typhimurium and *Listeria* monocytogenes ( $N=3$ ); (b) The relative change rate of impedance of the target bacteria, *E. coli* O157:H7, and the non-target bacteria, *Salmonella* typhimurium and *Listeria* monocytogenes ( $N=3$ ).

CFU/mL were prepared and magnetically separated, followed by detection at the optimal catalysis time of 5 min using this proposed impedance biosensor. The EIS of different concentrations of *E. coli* O157:H7 was shown in Fig. 5 (a). When the concentration of the target bacteria increased, the impedance of the supernatant decreased, indicating that more enzymatic bacteria were formed and thus more ammonium carbonate was produced. To further build up the calibration curve of this proposed biosensor, RZ at the characteristic frequency of 15 kHz were averaged and plotted with the concentration of *E. coli* O157:H7. As shown in Fig. 5(b), a good linear relationship between the relative change rate of impedance (RZ) and the concentration (C) of *E. coli* O157:H7 ranging from  $1.2 \times 10^1$  CFU/mL to  $1.2 \times 10^5$  CFU/mL was found and could be described as

$$RZ = 0.031\ln(C) + 0.449(R^2 = 0.95) \quad (3)$$

The detection limit of this proposed biosensor was determined by three times of signal-to-noise ratio and calculated as  $1.2 \times 10^1$  CFU/mL for the pure culture. The high sensitivity of this biosensor was due to the following reasons: (1) the impedance normalization with less variations resulting from the difference of the microelectrodes; (2) the higher concentration of the catalysate due to smaller microfluidic channel and thus less volume of urea for catalysis; and (3) the larger impedance change for different concentrations of the catalysate due to the continuous-flow measurement of the

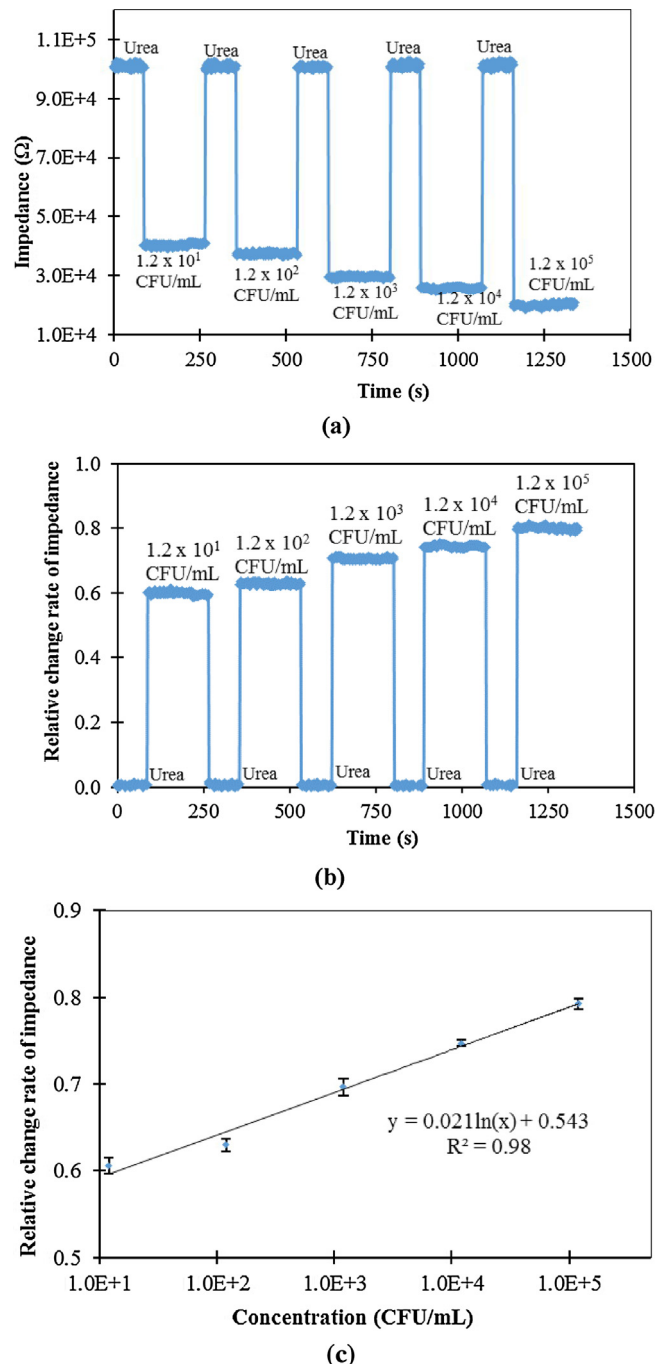


**Fig. 7.** (a) The impedance measured at the characteristic frequency of 15 kHz in the continuous-flow condition for *E. coli* O157:H7 with different concentrations ranging from  $1.2 \times 10^1$  CFU/mL to  $1.2 \times 10^5$  CFU/mL; (b) The relative change rate of impedance for *E. coli* O157:H7 with different concentrations ranging from  $1.2 \times 10^1$  CFU/mL to  $1.2 \times 10^5$  CFU/mL; (c) The linear relationship between the relative change rate of impedance measured at the characteristic frequency of 15 kHz and the concentration of *E. coli* O157:H7 in the spiked milk samples ( $N=3$ ).

impedance. Besides, the TEM imaging was used to verify the forming of the MNP-bacteria complexes and the MNP-bacteria-GNP complexes, as shown in Fig. 5 (c) and (d).

### 3.5. Specificity of this biosensor to non-target bacteria

The specificity of this proposed impedance biosensor mainly depends on the polyclonal antibodies against *E. coli* O157:H7 in

**Table 1**

Comparison of different data analysis methods.

Electrode	Zs (kΩ)	Zu (kΩ)	ΔZ (kΩ)	RZ
Electrode 1	37.1	46.0	8.9	0.19
Electrode 2	80.5	102.6	22.1	0.22
Electrode 3	43.5	54.9	11.4	0.21
Average	53.7	67.8	14.1	0.21
Standard deviation	23.4	30.4	7.0	0.01
Relative standard deviation	44%	45%	50%	5%

the forming of the magnetic bacteria and the aptamers against *E. coli* O157:H7 in the forming of the enzymatic bacteria. *Salmonella typhimurium* and *Listeria monocytogenes* at the same concentration level of  $10^4$  CFU/mL with *E. coli* O157:H7 were used as the non-target bacteria to test the specificity of this biosensor, respectively. Three parallel tests were conducted to test the specificity of the polyclonal antibodies. After the magnetic separation, both the original and magnetically separated bacteria were surface plated for bacterial enumeration, and the separation efficiency was defined as the ratio of the separated bacteria to the original ones. As shown in Fig. 6(a), the separation efficiency of *E. coli* O157:H7 at the concentration of  $1.2 \times 10^4$  CFU/mL is over 90%, however those of *Salmonella typhimurium* at the concentration of  $2.3 \times 10^4$  CFU/mL and *Listeria monocytogenes* at the concentration of  $2.1 \times 10^4$  CFU/mL were both less than 5%, indicating that the magnetic separation had a good specificity.

Besides, these three separated magnetic bacteria were used to react with the apta-urease GNPs, followed by urease catalysis and continuous-flow impedance measurement to obtain their relative change rates of impedance. As shown in Fig. 6(b), the relative change rate of impedance for *E. coli* O157:H7 was much higher than those of *Salmonella typhimurium* and *Listeria monocytogenes*, indicating that the specificity of this biosensor was further enhanced by the aptamers against *E. coli* O157:H7.

### 3.6. Comparison of different data analysis methods

To minimize the impedance difference of different microelectrodes, impedance normalization, i.e., the relative change rate of impedance at the characteristic frequency, was used to analyze the impedance data. To further verify this, the impedance of ammonium carbonate at the concentration of  $10 \mu\text{M}$  and the urea at the concentration of  $100 \mu\text{M}$  was measured by three different microelectrodes fabricated in the same batch at the characteristic frequency of  $15 \text{ kHz}$ . The standard deviation of their impedance of ammonium carbonate at the concentration of  $10 \mu\text{M}$  ( $Z_s$ ), their impedance changes ( $\Delta Z$ ) compared to the urea at the concentration of  $100 \mu\text{M}$  ( $Z_u$ ), and their relative change rates of impedance ( $RZ$ ) were calculated and compared. As shown in Table 1, both the standard deviation and the relative standard deviation of  $RZ$  were much less than those of  $\Delta Z$ , which was often used to calculate the concentration of the target bacteria. This indicated that this impedance normalization was effective to reduce the impact from the difference of the microelectrodes.

### 3.7. Detection of target bacteria in the spiked milk

To further evaluate the applicability of this proposed impedance biosensor for detection of the target bacteria in food sample, the pasteurized milk was purchased from local supermarket and 10 times diluted with the sterile PBS and then used to prepare the spiked milk samples with the *E. coli* O157:H7 concentrations ranging from  $1.2 \times 10^1$  CFU/mL to  $1.2 \times 10^5$  CFU/mL. Three parallel tests on different concentrations of *E. coli* O157:H7 in the spiked milk were conducted using the proposed magnetic separation and

Electrode	Channel	Detection time (min)	Linear range (CFU/mL)	Detection limit (CFU/mL)	Bacteria	Ref
IDME	No	30	$10^1$ – $10^4$	$3.0 \times 10^2$	Listeria	[20]
IDME	Yes	30	$10^1$ – $10^4$	$1.6 \times 10^2$	Listeria	[19]
SPIDE	No	30	$10^3$ – $10^4$	$1.6 \times 10^3$	Listeria	[21]
SPIDME	No	30	$10^2$ – $10^7$	$1.0 \times 10^2$	<i>E. coli</i>	[23]
SPIDME	No	45	$10^2$ – $10^6$	$2.0 \times 10^3$	<i>E. coli</i> / <i>Salmonella</i>	[12]
PCBIDE	Yes	15	$10^1$ – $10^5$	$1.2 \times 10^1$	<i>E. coli</i>	[22]
IDME	Yes	5	$10^1$ – $10^5$	$1.2 \times 10^5$	<i>E. coli</i>	This study

**Table 2**  
Comparison of this proposed biosensor with other electrochemical impedance biosensors for detection of foodborne pathogens.

impedance biosensor. The continuous-flow impedance of different concentrations of *E. coli* O157:H7 were shown in Fig. 7 (a) and the relative change rates of impedance were calculated and shown in Fig. 7 (b). As shown in Fig. 7 (c), the relative change rate of impedance measured at the characteristic frequency of 15 kHz had a good linear relationship with the concentration of the bacteria, which could be expressed as

$$RZ = 0.021\ln(C) + 0.543 \quad (R^2 = 0.98) \quad (4)$$

### 3.8. Comparison of this biosensor with previous reported biosensors

To further evaluate the performance of this proposed impedance biosensor, some recently reported impedance biosensors for detection of foodborne bacteria using different transducers, such as interdigitated microelectrode (IDME) [19,20], screen printed interdigitated electrode (SPIDE) [21], printed circuit board interdigitated electrode (PCBIDE) [22], screen printed interdigitated microelectrode (SPIDME) [12,23], were compared and shown in Table 2. This proposed biosensor had shown a shorter detection time and a lower detection limit than other reported biosensors due to the following reasons: (1) this biosensor used the urease to amplify the biological signals; (2) this biosensor used the continuous-flow impedance measurement to reduce the detection time and improve the sensitivity; (3) this biosensor used the impedance normalization to reduce the background noise from the variation of different microelectrodes.

## 4. Conclusion

In this study, we have successfully developed a microfluidic impedance biosensor combined magnetic separation and urease catalysis for continuous-flow detection of *E. coli* O157:H7, and demonstrated that the impedance normalization was effective to reduce the impact from the variation of different microelectrodes. This proposed biosensor had a good linear relationship between the relative change rate of impedance and the concentration of *E. coli* O157:H7 from  $10^1$  and  $10^5$  CFU/mL and was able to detect *E. coli* O157:H7 as low as  $1.2 \times 10^1$  CFU/mL in 2 h. More importantly, this microfluidic impedance biosensor has shown the potential to integrate with the fluidic immunomagnetic separation for online detection of foodborne pathogens and might be also extended to detect other foodborne pathogens using their specific antibodies and/or aptamers.

## Acknowledgments

This study was supported by the National Key Research and Development of China (2016YFD0500900) and Walmart Foundation (SA1703161).

## References

- [1] World Health Organization, 2017, <http://www.who.int/mediacentre/factsheets/fs399/en/>.
- [2] The U.S. Department of Agriculture, 2017. <http://www.cdc.gov/foodsafety/cdc-and-food-safety.html>.
- [3] National Healthy and Family Planning Commission, 2016, <http://www.nhfpc.gov.cn/yjb/s7859/201604/8d34e4c442c54d33909319954c43311c.shtml>.
- [4] C. Gilbert, A. O'Leary, D. Winters, M. Slavik, Development of a multiplex PCR assay for the specific detection of *Salmonella*, *campylobacter jejuni*, *escherichia coli* O157:H7, and *Listeria monocytogenes*, *Rapid Methods Autom. Microbiol.* 11 (2015) 61–74.
- [5] P. Truchado, M.I. Gil, T. Kostic, A. Allende, Optimization and validation of a PMA qPCR method for *Escherichia coli* quantification in primary production, *Food Control* 62 (2016) 150–156.
- [6] S. Shan, D. Liu, Q. Guo, S. Wu, R. Chen, K. Luo, L. Hu, Y. Xiong, W. Lai, Sensitive detection of *Escherichia coli* O157:H7 based on cascade signal amplification in ELISA, *J. Dairy Sci.* 99 (2016) 7025–7032.
- [7] X. Zhang, M. Li, B. Zhang, K. Chen, K. He, Development of a sandwich ELISA for *EHEC* O157:H7 intimin [gamma]1, *PLoS One* 11 (2016) e0162274.
- [8] J. Khang, D. Kim, K.W. Chung, J.H. Lee, Chemiluminescent aptasensor capable of rapidly quantifying *Escherichia coli* O157:H7, *Talanta* 147 (2016) 177–183.
- [9] B. Balakrishnan, S. Barizuddin, T. Wuliji, M. El-Dweik, A rapid and highly specific immunofluorescence method to detect *Escherichia coli* O157:H7 in infected meat samples, *Int. J. Food Microbiol.* 231 (2016) 54–62.
- [10] L. Xu, Z. Lu, L. Cao, H. Pang, Q. Zhang, Y. Fu, Y. Xiong, Y. Li, X. Wang, J. Wang, Y. Ying, Y. Li, In-field detection of multiple pathogenic bacteria in food products using a portable fluorescent biosensing system, *Food Control* 75 (2017) 21–28.
- [11] A. Pandey, Y. Gurbuz, V. Ozguz, J.H. Niazi, A. Qureshi, Graphene-interfaced electrical biosensor for label-free and sensitive detection of foodborne pathogenic *E. coli* O157:H7, *Biosens. Bioelectron.* 91 (2017) 225–231.
- [12] M. Xu, R. Wang, Y. Li, Rapid detection of *Escherichia coli* O157:H7 and *Salmonella Typhimurium* in foods using an electrochemical immunosensor based on screen-printed interdigitated microelectrode and immunomagnetic separation, *Talanta* 148 (2016) 200–208.
- [13] L. Guo, S. Zhi, X. Sun, C. Lei, Y. Zhou, Ultrasensitive detection of bioanalytes based on signal amplification of coil-integrated giant magnetoimpedance biosystems, *Sens. Actuators B-Chem* 247 (2017) 1–10.
- [14] X. Sun, C. Lei, L. Guo, Y. Zhou, Separable detecting of *Escherichia coli* O157:H7 by a giant magneto-resistance-based bio-sensing system, *Sensor Actuators B-Chem* 234 (2016) 485–492.
- [15] V.C. Ozalp, G. Bayramoglu, Z. Erdem, M.Y. Arica, Pathogen detection in complex samples by quartz crystal microbalance sensor coupled to aptamer functionalized core-shell type magnetic separation, *Anal. Chim. Acta* 853 (2015) 533–540.
- [16] L. Wang, R. Wang, F. Chen, T. Jiang, H. Wang, M. Slavik, H. Wei, Y. Li, QCM-based aptamer selection and detection of *Salmonella typhimurium*, *Food Chem.* 221 (2017) 776–782.
- [17] T. Nguyen, K. Trinh, W. Yoon, N. Lee, H. Ju, Integration of a microfluidic polymerase chain reaction device and surface plasmon resonance fiber sensor into an inline all-in-one platform for pathogenic bacteria detection, *Sens. Actuators B-Chem.* 242 (2017) 1–8.
- [18] X. Liu, Y. Hu, S. Zheng, Y. Liu, Z. He, F. Luo, Surface plasmon resonance immunosensor for fast, highly sensitive, and in situ detection of the magnetic nanoparticles-enriched *Salmonella enteritidis*, *Sens. Actuators B-Chem.* 230 (2016) 191–198.
- [19] Q. Chen, D. Wang, G. Cai, Y. Xiong, Y. Li, M. Wang, et al., Fast and sensitive detection of foodborne pathogen using electrochemical impedance analysis, urease catalysis and microfluidics, *Biosens. Bioelectron.* 86 (2016) 770–776.
- [20] Q. Chen, J. Lin, C. Gan, Y. Wang, D. Wang, Y. Xiong, et al., A sensitive impedance biosensor based on immunomagnetic separation and urease catalysis for rapid detection of *Listeria monocytogenes* using an immobilization-free interdigitated array microelectrode, *Biosens. Bioelectron.* 74 (2015) 504–511.
- [21] D. Wang, Q. Chen, H. Huo, S. Bai, G. Cai, W. Lai, et al., Efficient separation and quantitative detection of *Listeria monocytogenes* based on screen-printed interdigitated electrode, urease and magnetic nanoparticles, *Food Control* 73 (2017) 555–561.
- [22] L. Wang, L. Xue, F. Huang, H. Zhang, G. Cai, J. Lin, An electrochemical aptasensor using coaxial capillary with magnetic nanoparticle, urease catalysis and PCB electrode for rapid and sensitive detection of *Escherichia coli* O157:H7, *Nanotheranostics* 1 (2017) 403–414.
- [23] Z. Li, Y. Fu, W. Fang, Y. Li, Electrochemical impedance immunosensor based on self-assembled monolayers for rapid detection of *Escherichia coli* O157:H7 with signal amplification using lectin, *Sens.-Basel* 15 (2015) 19212–19224.

## Biographies

**Miss Lan Yao** is now a master student at the Department of Electronic Engineering, China Agricultural University in Beijing, China. She got her bachelor degree of Electronic Engineering in 2017 at China Agricultural University. She started her research on electrochemical impedance biosensor and immunomagnetic separation for bacteria detection with Dr. Jianhan LIN at China Agricultural University since October 2016. Her current research interests include electrochemical biosensors and magnetic separation for detection of pathogenic microorganisms in foods, as well as portable bio-instruments for in-field detection of foodborne pathogens, etc.

**Miss Lei Wang** is now a Ph.D. student at the Department of Electronic Engineering, China Agricultural University in Beijing, China. She got her bachelor degree of Electrical Engineering in June 2016 in Hebei Agricultural University. She started her Doctoral Research on impedance biosensors with Dr. Jianhan LIN at China Agricultural University since September 2016. Her current research interests include various biosensors for rapid and sensitive detection of pathogenic microorganisms in food or animal samples, etc.

**Miss Fengchun Huang** is now a Ph.D. student at the Department of Electronic Engineering, China Agricultural University in Beijing, China. She got her bachelor degree of Microbiology in 2014 in Fujian Agriculture and Forestry University and Master degree of Food Science in Nanchang University in 2016. She started her Doctoral Research on impedance and optical biosensors with Dr. Jianhan LIN at China Agricultural University since September 2016. Her current research interests include nanomaterials and biosensing methods for rapid and sensitive detection of pathogenic microorganisms in food or animal samples, etc.

**Mr. Gaozhe CAI** is now a Ph.D. student at the Department of Electronic Engineering, China Agricultural University in Beijing, China. He got his bachelor degree of Electronic Engineering in 2015. He started his Doctoral Research on biosensors and microfluidic biochips with Dr. Jianhan LIN at China Agricultural University since September 2015. His current research interests include microfluidic chips for separation and detection of pathogenic microorganisms in food or animal samples, microfluidic simulation, as well as portable bio-instrumentation for in-field detection of foodborne pathogens, etc.

**Miss Xinge Xi** is now a Ph.D. student at the Department of Biological and Agricultural Engineering, University of Arkansas at Fayetteville, AR, USA. She got her bachelor degree of Electronic Engineering in June 2017 at China Agricultural University and started her research on electrochemical and optical biosensors for detection of foodborne bacteria with Dr. Yanbin LI at the University of Arkansas since August 2017. Her current research interests include electrochemical and optical biosensors for rapid detection of pathogenic bacteria in foods.

**Dr. Jianhan LIN** is now an Associate Professor at the Department of Electronic Engineering, China Agricultural University in Beijing, China. He got his bachelor degree of Electronic Engineering in 2001, master degree and Ph. D. degree of Agricultural Engineering in 2004 and 2007 supervised by Academician/Prof. Maohua WANG at China Agricultural University. He started his Postdoctoral Research in Biological Engineering with Prof. Yanbin LI at the University of Arkansas at Fayetteville, Arkansas, US from October 2007 to May 2009, and worked as Research Associate at the University of Arkansas from June 2009 to June 2011. Then, he was appointed as Chief Technology Officer by Aibit Biotech LLC at Wuxi, China in July 2011 and joined China Agricultural University since September 2012. His current research interests include biosensors for rapid detection of foodborne pathogens and animal diseases, microfluidic chip for separation and detection of biological and chemical analyte, food supply chain management and traceability, as well as infectious animal disease prevention and control, etc. So far, he has published more than 30 peer review papers in Biosensors & Bioelectronics, Food Control, Journal of Separation Sciences, etc. and filed 10 patents.